Biochimica et Biophysica Acta 1837 (2014) 1635–1642

Contents lists available at ScienceDirect

Biochimica et Biophysica Acta

journal homepage: www.elsevier.com/locate/bbabio

The ultrastructure of *Chlorobaculum tepidum* revealed by cryo-electron tomography

Misha Kudryashev [a,b], Aikaterini Aktoudianaki [c], Dimitrios Dedoglou [c], Henning Stahlberg [a], Georgios Tsiotis [c,*]

[a] Center for Cellular Imaging and NanoAnalytics (C-CINA), Biozentrum, University of Basel, 4058 Basel, Switzerland
[b] Focal Area Infection Biology, Biozentrum, University of Basel, 4058 Basel, Switzerland
[c] Division of Biochemistry, Department of Chemistry, University of Crete, 71003 Voutes, Heraklion, Greece

ARTICLE INFO

Article history:
Received 19 March 2014
Received in revised form 4 June 2014
Accepted 10 June 2014
Available online 17 June 2014

Keywords:
Electron microscopy
Cryo-electron tomography
Green sulfur bacteria
Chlorosome

ABSTRACT

Chlorobaculum (*Cba*) *tepidum* is a green sulfur bacterium that oxidizes sulfide, elemental sulfur, and thiosulfate for photosynthetic growth. As other anoxygenic green photosynthetic bacteria, *Cba tepidum* synthesizes bacteriochlorophylls for the assembly of a large light-harvesting antenna structure, the chlorosome. Chlorosomes are sac-like structures that are connected to the reaction centers in the cytoplasmic membrane through the BChl *a*-containing Fenna–Matthews–Olson protein. Most components of the photosynthetic machinery are known on a biophysical level, however, the structural integration of light harvesting with charge separation is still not fully understood. Despite over two decades of research, gaps in our understanding of cellular architecture exist. Here we present an in-depth analysis of the cellular architecture of the thermophilic photosynthetic green sulfur bacterium of *Cba tepidum* by cryo-electron tomography. We examined whole hydrated cells grown under different electron donor conditions. Our results reveal the distribution of chlorosomes in 3D in an unperturbed cell, connecting elements between chlorosomes and the cytoplasmic membrane and the distribution of reaction centers in the cytoplasmic membrane.

1. Introduction

Green sulfur bacteria (GSB; order *Chlorobia*) are anerobic, photosynthetic bacteria that utilize reduced sulfur compounds as electron donors to a photosynthetic electron transport chain. The chain provides energy and reduced ferredoxin to drive carbon fixation, biosynthesis, and cell growth [1,2]. *Chlorobia* are widely distributed in aquatic environments where anoxic layers containing reduced sulfur compounds are exposed to light. They predominantly utilize sulfide (S^{2-}), thiosulfate ($S_2O_3^{2-}$), biogenic and abiogenic sulfur (S^0) globules, and hydrogen (H_2) as electron donors to support photoautotrophic growth [3]. Most strains can oxidize S^{2-} and H_2, while oxidation of $S_2O_3^{2-}$ is less commonly encountered in cultivated strains. *Chlorobia* are known to have a high affinity for S^{2-}, and this is usually the preferred substrate. Initially, S^{2-} is generally incompletely oxidized to S^0, which is deposited extracellularly, and oxidized completely to sulfate (SO_4^{2-}) when all of the S^{2-} has been consumed [4]. At present, the mechanisms involved in the formation and consumption of S^0 in *Chlorobia* are largely unknown [5]. *Chlorobaculum* (*Cba*) *tepidum* TLS was isolated from a hot spring in New Zealand and like other *Chlorobia* preferentially oxidizes sulfide to S^0, which is deposited outside of the cell [6]. The ability of *Cba tepidum* to fix atmospheric nitrogen and its dependence on sulfur compounds for the photosynthetic processes, make this species an important model to understand the role microbes play in global nutrient cycles.

Being a Gram negative bacterium, *Cba tepidum* has an outer membrane (OM) and an inner cytoplasmic membrane (CM). The reaction center (RC), which is located in the CM, converts light energy into redox chemical energy, which is further transformed into stable oxidants and reductants [7]. The critical role that the cytoplasmic membrane plays in housing the photosynthetic and respiratory complexes, maintaining a proton gradient for the production of ATP, and maximizing light capture, makes the membrane architecture of *Cba tepidum* of particular interest [8]. Light is primarily captured by chlorosomes, which serve as huge antenna complexes. Chlorosomes are attached to the inner face of the CM and interact with the membrane-embedded RCs (reviewed in [9]) *via* the water-soluble Fenna–Matthews–Olson (FMO) proteins. The latter ~40 kDa protein is present as a homotrimer and associated with bacteriochlorophyll *a* (BChl *a*) [7,10–12]. Chlorosomes are ellipsoid organelles with an interior of self-organized BChl oligomers (BChl *c* and/or *d* or *e*; reviewed in [13]) contained by a

Abbreviations: AFM, atomic force microscopy; 3D, three dimensional; BChl, bacteriochlorophyll; *Cba*, *Chlorobaculum*; CM, cytoplasmic membrane; Cryo-ET, cryo-electron tomography; DLS, dynamic light scattering; EM, electron microscopy; FMO, Fenna–Mathew–Olson; GSB, green sulfur bacteria; OM, outer membrane; PFT-AFM, peak force tapping atomic force microscopy; PG, peptidoglycan; RC, reaction center; TEM, transmission electron microscopy

* Corresponding author at: Division of Biochemistry, Department of Chemistry, University of Crete, P. O. Box 2208, GR-71003 Voutes, Greece. Tel.: +30 2810 545006; fax: +30 2810 545001.
E-mail address: tsiotis@chemistry.uoc.gr (G. Tsiotis).

http://dx.doi.org/10.1016/j.bbabio.2014.06.002
0005-2728/

lipid envelope. They have a specific region termed the baseplate comprised of primarily CsmA-BChl *a* protein–pigment complexes organized in a two dimensional paracrystalline array [14]. Baseplates are exclusively located on the chlorosome surface facing the CM [15], into which the C-terminus of CsmA is thought to insert [16]. The N-terminus of the CsmA proteins is inserted in the lipid monolayer of the chlorosome envelope [16].

Various attempts have been made to visualize structural details of the light harvesting and energy transfer-mediating systems of *Chlorobia*. The 2.2 Å crystal structure of the FMO protein has trimeric crystallographic symmetry [10]. Single particle electron microscopy (EM) has given structural information for *Cba tepidum* RC core complexes, RCs associated with FMO protein and FMO protein complexes [11,12,17]. Chlorosomes isolated from *Cba tepidum* have been investigated using EM, light scattering and proteomics tools [13,18] and the structure of the FMO protein is available at 1.9 Å resolution [19]. Cryo-EM and X-ray scattering indicate a lamella organization of pigments within chlorosomes [20–22]. Isolated chlorosomes from three different phyla, *Chloroflexus aurantiacus*, *Cba tepidum* and the newly discovered *Candidatus Chloracidobacterium thermophilum* have also been analyzed under close to native conditions using peak force tapping atomic force microscopy (PFT-AFM) [23].

To date, descriptions of the localization of chlorosomes relative to the CM and the organization of the OM and CM of the whole bacterium, are based on thin-section electron micrographs, freeze–fracture studies [8,24] and mass spectroscopy-based methods [25]. The first studies employed the freeze–fracture technique to investigate the photosynthetic machinery of *Chlorobium limicola* [26]. Some replicas revealed 10 nm-wide rod-like elements arranged in hexagonal arrays. Others showed regularly spaced planar arrays that were associated with the CM and often with the rod-like structures. Later work employing a different sample fixation protocol, reported that the interface between chlorosomes and the CM is occupied by repetitive structural elements [24]. These structures were shown to connect the chlorosomes to the CM, creating a space between them. Further, elements connecting the CM and the OM in the periplasmic space under the chlorosomes were also observed [24]. However, such studies have led to conflicting interpretations because the data were obtained by a variety of fixation techniques and protocols.

3D electron tomographic (ET) imaging of non-fixed, non-stained, hydrated biological material has allowed insights into the *in situ* organization of cells at macromolecular resolution [27,28]. Examination of chlorosomes isolated from *C. aurantiacus* (green nonsulfur bacteria) by cryo-ET confirmed the overall dimensions estimated by cryo-EM, but did not reveal internal structural details [21].

In the present paper, we use cryo-ET to define the three dimensional (3D) organization of the green sulfur bacterium *Cba tepidum* grown in the presence of sulfide (S^{2-}) and thiosulfate ($S_2O_3^{2-}$). Further, we employ cryo-ET to systematically analyze cellular structures of bacteria grown in the presence of S^{2-} alone.

2. Materials and methods

2.1. Culture media and growth

Cba tepidum was cultured as described previously [6]. The medium contained 7.7 mM Na_2S (S^{2-}) and 4 mM $Na_2S_2O_3 \cdot 5H_2O$ ($S_2O_3^{2-}$) as electron donors. Cultures (1 L or 500 mL) were incubated at 47 °C under continuous illumination from 2 W illuminating tubes at 20 μE m^{-2} s^{-1}. Cells were harvested 1–2 days after inoculation with 20 mL of old cell culture.

2.2. Sulfide transition

Cultures were inoculated into 500 mL of medium as described previously [6] except that $S_2O_3^{2-}$ was omitted. The concentration of S^{2-} was 9.5 mM. Cultures were incubated at 47 °C under continuous illumination from 20-W illuminating tubes at 20 μE m^{-2} s^{-1}. Cells were harvested 1–2 days after inoculation with 20 mL of cells cultured in the presence of 7.7 mM S^{2-} and 4 mM $S_2O_3^{2-}$.

S^0 and BChl *c* were determined spectrophotometrically. The cell pellet was extracted with methanol, and the concentrations in the supernatant were determined at 265 nm and 669 nm, respectively, using absorption coefficients of 23.9 L g^{-1} cm^{-1} [29] and 86 L g^{-1} cm^{-1} [30]. S^{2-} was measured using the colorimetric methylene blue method [31]. SO_4^{2-} was measured by ion chromatography using a Dionex AG4A-SC 4 mm pre-column and a Dionex AS4A-SC 4 mm column attached to a Dionex GP50 gradient pump. The column was equilibrated by a buffer containing 3.4 mM $NaHCO_3$ and 3.6 mM Na_2CO_3, at 1.5 mL/min. SO_4^{2-} was detected by a Dionex CD20 conductivity detector.

2.3. Cryo-ET

Cryo-electron tomography (cryo-ET) was performed essentially as described before [32]. Bacteria in their respective growth medium were anerobically centrifuged for 3 min at 300 *g*. The pellet containing ~20 μL of media was mixed with 1 μL of 10 nm colloidal gold particles and rapidly transferred onto glow-discharged holey carbon Quantifoil EM grids. Grids were rapidly plunge frozen in liquid ethane cooled to liquid nitrogen temperature, using a Vitrobot (FEI Corp, Hillsboro, USA). The grids were observed in a Titan Krios (FEI) operating at 300 kV and equipped with a Gatan post column energy filter and a 2 k Ultrascan 1000 CCD camera (Gatan, Pleasanton, USA). Single axis tilt series were acquired with an increment of 2° covering −60° to +60°. The cumulative dose was under 10,000 electrons/nm^2 and the defocus was −5 to −10 μm.

A total of 19 tomographic tilt series were recorded for *Cba tepidum* grown in the presence of S^{2-} and $S_2O_3^{2-}$ and 6 tomographic tilt series for *Cba tepidum* grown in the presence of just S^{2-}. The tomograms were reconstructed by weighted back-projection using the *eTomo* (Boulder Laboratory for 3D Electron Microscopy) [33]. Volume-rendered segmentation were performed manually using the Amira package (FEI Corp., Hillsboro, USA).

2.4. Connections between the IM and chlorosomes

198 sub-volumes from 2 × 2 × 2 voxel binned volumes (resulting pixel size = 1.08 nm) were extracted from 8 tomograms of bacteria grown in the presence of S^{2-} and $S_2O_3^{2-}$ and recorded at a defocus of −5 μm. The particles were manually translationally and rotationally aligned to a common center and orientation using the dynamo_gallery tool of Dynamo (www.dynamo-em.org) [34]. The particles then were separated to the even and odd subpopulations and processed independently: the particles were aligned to a template that was generated summing up the manually aligned particles. The average was iteratively refined applying high rotational symmetry; the final resolution was obtained by measuring Fourier ring correlation between the final averages from the odd and even subpopulations, using the 0.143 threshold criterion. No correction for the contrast transfer function was performed, as it was not limiting for the resolution [35].

3. Results

In *Cba tepidum* cultures that contain both S^{2-} and $S_2O_3^{2-}$, S^{2-} is oxidized preferentially and S^0 globules are formed [4]. Following S^{2-} depletion, $S_2O_3^{2-}$ and S^0 globules are oxidized to SO_4^{2-}. In order to study whether the presence of $S_2O_3^{2-}$ affects the formation of S^0 globules, we grew the bacteria in the presence of both S^{2-} and $S_2O_3^{2-}$ and in the presence of just S^{2-}. The amount of S^{2-} ions initially present was the same in both cases. Fig. 1A shows the growth rate of the bacterial cells indicated by the BChl *c* concentration. At the same time, we measured the transformation of the sulfur compounds to SO_4^{2-}, which is

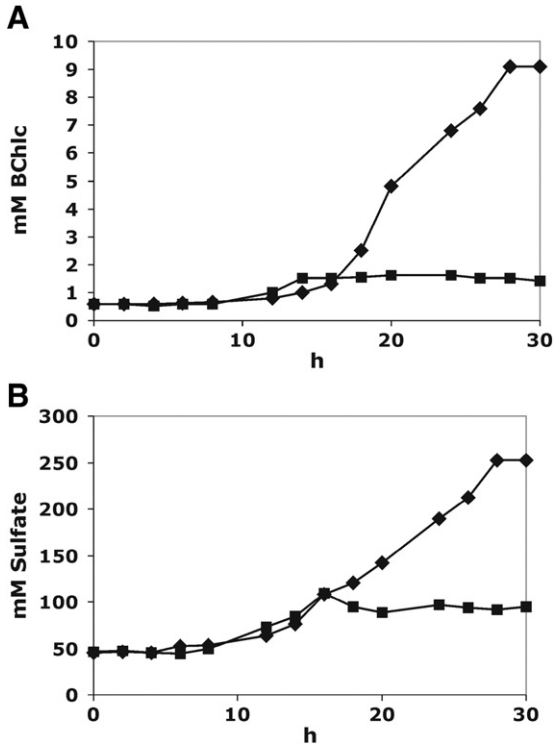

Fig. 1. Influence of culture conditions on the growth of *Cba tepidum* and sulfur oxidation. A. BChl *c* concentration during the growth of *Cba tepidum* in S^{2-} and $S_2O_3^{2-}$ (rhombus) and in just sulfide S^{2-} (rectangle). The initial BChl *c* concentration is attributed to the inoculated *Cba tepidum* cells. About 16 h after culture initiation, the growth rates start to vary. Proliferation is slower in the absence of $S_2O_3^{2-}$ (B). Transformation of sulfur compounds to SO_4^{2-} in a 1-L culture of *Cba tepidum* grown in S^{2-} and $S_2O_3^{2-}$ (rhombus) and only in sulfide S^{2-} (rectangle). The initial SO_4^{2-} concentration (50 mM) is attributed to the SO_4^{2-} content of the growth medium. The production of SO_4^{2-} correlates to the number of bacteria present.

the highest oxidation state of sulfur (Fig. 1B). There is a clear correlation between the number of bacteria and the production of SO_4^{2-}, regardless of whether $S_2O_3^{2-}$ was initially present in the medium or not. After about 16 h, growth of the bacteria becomes much slower in the absence of $S_2O_3^{2-}$ and is consequently affected that the SO_4^{2-} concentration is lower.

Anerobically and photoheterotropically cultured *Cba tepidum* cells were cultured for 20 h in the presence of S^{2-} with and without $S_2O_3^{2-}$ and visualized by cryo-EM and cryo-ET (Fig. 2). The overall size of *Cba tepidum* grown in both conditions were similar. Despite their relatively large diameter (500–600 nm), the bacteria were only a few hundred nanometers thick allowing *in situ* visualization. The OM and CM could be distinguished as well as the chlorosome arrangement on the inner side of the CM (Fig. 2C and D). Following the electron density variations from the outside towards the inside of the cell (Fig. 2E) further documents these features and their dimensions. The distance between the OM and the CM is about 30 nm for *Cba tepidum* grown in media containing both sulfur compounds. Interestingly, the OM–CM separation was variable and could increase to 65 nm in bacteria grown in S^{2-} alone (Fig. 2B). In addition, the peptidoglycan (PG) layer can be discerned (Fig. 2A–C). Bacteria grown only in S^{2-} regularly contained electron dense inclusions of various sizes, $r = 96 \pm 22$ nm (Fig. 2D). These structures look similar to the phosphorous containing densities previously observed in electron micrographs of *Cba tepidum* [24]. Unfortunately, elemental analysis by electron energy loss spectroscopy (EELS) did not give a reliable estimate of their composition. For both, bacteria grown in the presence or in the absence of $S_2O_3^{2-}$, we were unable to identify sulfur globules outside of the bacterial cells in our EM tomograms.

Chlorosomes can be distinguished close to the inner side of the CM of bacteria grown under both conditions; they have a roughly oval cross-section and uniform electron density (Fig. 2C, D). Their length and width are not uniform, and vary in agreement with the reported size of isolated chlorosomes (see Table 1 and below). Connections between the chlorosomes and the CM can be seen in the tomograms (Fig. 2C).

In order to determine the architecture of the *Cba tepidum* RC *in situ*, we concentrated on the densities connecting the chlorosomes to the CM, assuming these to be formed by the RC-associated FMO complex [11,12] and domains of CsmA. We computationally extracted 198 tomographic volumes containing these densities and performed sub-volume averaging using the *Dynamo* pipeline [34]. The low signal-to-noise ratio of the small connecting elements did not allow their structure to be determined, as the alignment of the sub-volumes was dominated by the electron-dense membranes. The final average structure had a resolution of 4.3 nm (see Materials and methods). The average separation of the chlorosome envelope and the CM at these points was 8.5 nm (*i.e.*, the center-to-center distance between the CM and the chlorosome envelope; Fig. 2F); the width of the connecting element is ~8 nm (*i.e.*, the *f*ull *w*idth *h*alf *m*aximum (FWHM) of the electron density between the CM and the chlorosome envelope). The CM is 4 nm thick, which is the thickness of a lipid bilayer. The chlorosome envelope is half as thick (Fig. 2F), indicating that this membrane is formed by a single lipid monolayer in agreement with the structure proposed by Frigard and Bryant [15]. Taking in account the thickness of the CM and chlorosome envelope, we estimated that the distance between the CM surface and the chlorosome is about 6.5 nm.

Volume rendering of the two bacteria shown in Fig. 2 provides an overall view of their internal organization (Fig. 3). The reconstructed image allows the distribution of the connections between the chlorosomes and the RCs located in the CM to be analyzed in detail for bacteria grown in S^{2-} and $S_2O_3^{2-}$ (Fig. 3A) and in S^{2-} alone (Fig. 3B). The bacterial membranes on the top and the bottom of the cells are not resolved in tomograms due to the 'missing wedge' problem in electron tomography [28]. However investigation of 3D volumes showed that all the chlorosomes were close to the membranes. The distribution of chlorosomes is reported here for the first time for *Cba tepidum* cells (Fig. 4B). The lateral distance between the connecting proteins varies, however they tend to cluster closer than 20 nm (Fig. 4B) and in some regions seem to form a regular array (Fig. 4A, central panel). The average distances are 17.6 ± 10.6 and 15.4 ± 10.6 nm for bacteria grown in S^{2-} and $S_2O_3^{2-}$ and in S^{2-} alone correspondingly. Notably, the number of connections detected per chlorosome also varies.

As documented in Fig. 5, volume rendering shows that chlorosomes cover approximately 70% (±~20%) of the surface of the CM (the tomographic missing wedge prohibited higher precision) for *Cba tepidum* cells grown in the presence of S^{2-} and $S_2O_3^{2-}$ (Fig. 5) and is roughly the same when $S_2O_3^{2-}$ is not present (Fig. 2D and 3B). In both cases, they appear as approximately ellipsoidal objects with ruffled edges. The chlorosomes measured were 188 ± 85 nm long ($n = 65$), 98 ± 37 nm wide ($n = 134$) and 34 ± 13 nm thick ($n = 144$) when the bacteria were grown in S^{2-} and $S_2O_3^{2-}$ and 185 ± 58 nm long ($n = 113$), 70 ± 18 nm wide ($n = 72$) and 34 ± 8 nm thick ($n = 48$) when only S^{2-} was present in the growth medium (Fig. 5). The measurements were made on 8 tomograms of bacteria grown in S^{2-} and $S_2O_3^{2-}$ and 3 tomograms of bacteria grown in S^{2-}. These values are compared with data from the literature in Table 1. Based on these dimensions the average volume of one chlorosome in *Cba tepidum* cells is 314,000 nm^3 when S^{2-} and $S_2O_3^{2-}$ are present in the culture medium and 230,000 nm^3 when only S^{2-} is present (Table 1).

4. Discussion

It has been proposed that the ancestral photoautotroph was a green-sulfur bacterium [36]. Our cryo-ET data allow a comprehensive analysis of the cell organization of the green sulfur bacterium *Cba tepidum*. The computed tomographic volumes complement conventional electron micrographs of the *Cba tepidum* cell [24], and give a more complete

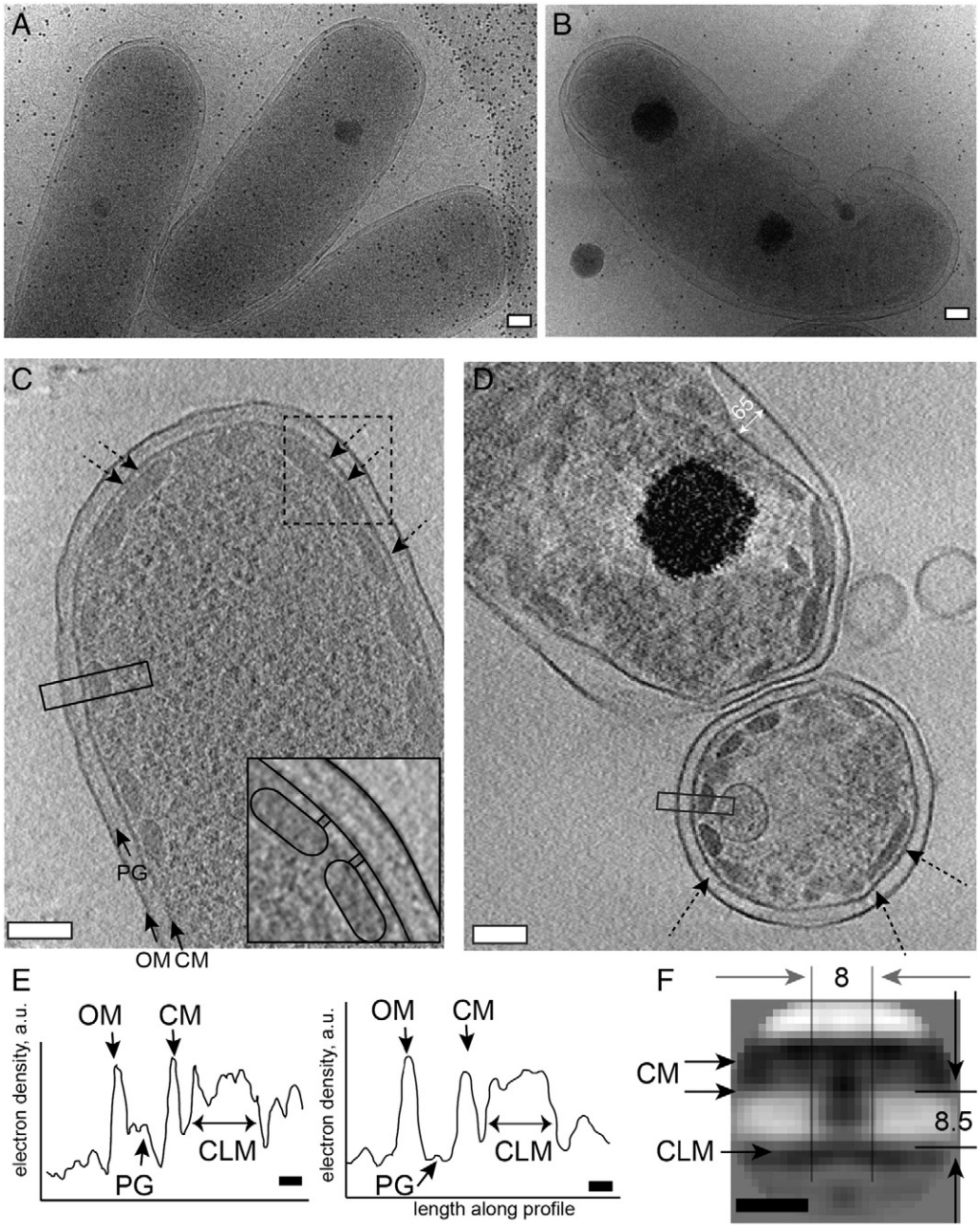

Fig. 2. Cryo-electron tomography of an intact *Cba tepidum* cell. A) A cryo-electron micrograph of typical cells grown in the presence of S^{2-} and $S_2O_3^{2-}$. B) A cryo-electron micrograph of typical cells grown in S^{2-} alone. C) A 20 nm thick x–y slice through a typical tomogram of the cell grown in the presence of S^{2-} and $S_2O_3^{2-}$. Inset shows a model magnified from the dashed rectangle. D) Corresponding slice for a cell grown in S^{2-} alone. Black arrows indicate the peptidoglycan layer (PG), outer membrane (OM) and cytoplasmic membrane (CM) and dotted arrows the connection of the chlorosome to the CM. White arrow indicates an increased distance between the OM and CM, measurement is in nm. E) Representative longitudinal electron density profile along the boxes in C (left) and D (right): columns of 40 nm from a 20 nm thick section were summed. Positions of the OM, CM, PG and chlorosome (CL) are indicated. F) An average structure of the CM–chlorosome connections derived by sub-tomogram averaging. The CM and CL membrane (CLM) are indicated, dimensions are given in nm. Scale bars: white 100 nm, black 10 nm.

view of the cellular ultrastructure of an anoxygenic photosynthetic prokaryote than presently available. Importantly, sample preparation only involved freezing the bacteria in a thin layer of vitreous ice, allowing intact cells to be examined in a hydrated state without the use of chemical fixatives or contrast enhancing stains. The reconstructed 3D organization of chlorosomes may serve as a baseline for further comparison between *Cba tepidum* and other strains of the green sulfur phylum.

The cell wall of Gram-negative bacteria is composed of an inner CM and an OM separated by a PG layer containing periplasma [8]. Our results clearly reveal these three layers without connections between the OM and IM (Figs. 2–3). In contrast connections between the CM and the OM have been reported previously, but it is unclear whether these are formed by proteins or membranous structures [24].

Cba tepidum, a strictly anerobic photosynthetic bacterium, oxidizes S^{2-}, S^0, and $S_2O_3^{2-}$ for use as an electron donor in its photosynthesis [6]. In the presence of S^{2-} and $S_2O_3^{2-}$, S^{2-} is oxidized preferentially and S^0 globules are formed [4]. Following S^{2-} depletion, $S_2O_3^{2-}$ and S^0 globules are oxidized to SO_4^{2-} [4]. The exact structure of this S^0 is still debated, but it is thought to occur as long-chain, zero-valent polysulfanes, probably terminated by organic residues [37]. In anoxygenic phototrophic sulfur bacteria, S^0 is generally deposited outside of the cell cytoplasm, sometimes in the periplasm and sometimes

Table 1
Comparison of reported dimensions for chlorosomes from *Cba tepidum*.

Sample	Treatment	Technique	Average dimensions			Ratio L/W	Volume $* 10^3$ nm^3	Surface area $* 10^3$ nm^2	Reference
			L nm	W nm	H nm				
Whole cells	Thin-sectioned	TEM	100–180	40–60	40–60	2.8	183	14*	[6]
Isolated chlorosomes	Dried	TM-AFM	194	104	26	1.9	274*	65*	[44]
Isolated chlorosomes	Dried	TM-AFM	174	91	11	1.9	91	505*	[48]
Isolated chlorosomes	Cryo-frozen	Cryo EM	140–180	50	–	1.7	–	–	[22]
Isolated chlorosomes		AFM	212	122	35	1.7	474	84*	[15]
Isolated chlorosomes	Buffered liquid	PFT-AFM	133	57	36	2.3	141	25*	[23]
Isolated chlorosomes	Negative stain	TEM	149	52	–	2.8	–	–	[18]
Isolated chlorosomes	Freeze-drying	STEM	147	51	–	2.8	–	–	[18]
Isolated chlorosomes	Buffered liquid	DLS	136	90	–	1.5	–	–	[18]
Whole cells (S^{2-}, $S_2O_3^{2}$)	Vitrified	Cryo-ET	188 ± 85	98 ± 37	34 ± 13	1.9	314*	57*	This study
Whole cells (S^{2-})	Vitrified	Cryo-ET	185 ± 58	70 ± 18	34 ± 8	2.8	230*	42*	This study

* Values were calculated in this manuscript; when the range of the dimensions was given the average value was used. For the calculation of volumes and surface areas chlorosomes were assumed ellipsoidal with axis L, W, H. Volume is calculated as $V = 4 / 3\pi * a * b * c$. Surface was calculated as $S = 4\pi * ((a^p * b^p + a^p * c^p + b^p * c^p) / 3)^{1/p}$, where $a = L / 2$; $b = W / 2$, $c = H / 2$, $p = 1.6075$.

outside the cell wall. Just how organisms that 'store' S^0 outside the cell wall access this source of reductant remains an open question. However, S^0 produced by S^{2-}-limited continuous cultures of *Cba thiosulfatiphilum* seems to remain attached to the cells [38]. Although S^0 globules were not visible in our EM-tomograms, the increased distance between the OM and CM often observed when bacteria were grown in the presence of S^{2-} alone hints that under these conditions the bacteria might store S^0 in the periplasmatic space. The elemental composition of the inclusions present in many of these bacteria grown in the presence of S^{2-} could not be determined. They might be formed by S^0-related deposits, or be phosphorous containing, as previously suggested for densities in *Cba tepidum* [24].

In green sulfur bacteria, the CM is critical for photosynthesis and some fundamental metabolic processes [39]. In addition to the RC complexes, it contains the cytochrome *bc* complex, ATP synthase and enzymes involved in the oxidative sulfur metabolism [7,40,41]. In the process of photosynthesis, energy absorbed by chlorosomes is transferred *via* the FMO protein to the RC, where charge separation occurs [7,14]. Chlorosomes, the largest photosynthetic light-harvesting antenna complexes known, are attached to the cytoplasmic side of the CM [15]. They contain more than 250,000 BChl pigments densely packed in concentric coaxial nanotubes [42], which results in the highly efficient capture of light energy. A series of functional and structural studies has been made [11,12,21,23]. Relevant to this work, the size of *Cba tepidum* chlorosomes has been determined by various methods such as DLS, TEM and AFM (Table 1). These techniques have yielded dimensions that differ by a factor of two (Table 1) [18,23,43–45]. Extraction from the cell, adsorption to a carbon layer, drying or dehydration and embedding in resin for sectioning could all affect chlorosome size and cause the significantly smaller dimensions measured in several cases for isolated chlorosomes. Our study emphasizes the importance of imaging chlorosomes in their native, hydrated form without isolation, staining, or drying [23]. Further, we found that chlorosomes from cells growing in different conditions have a significantly different width

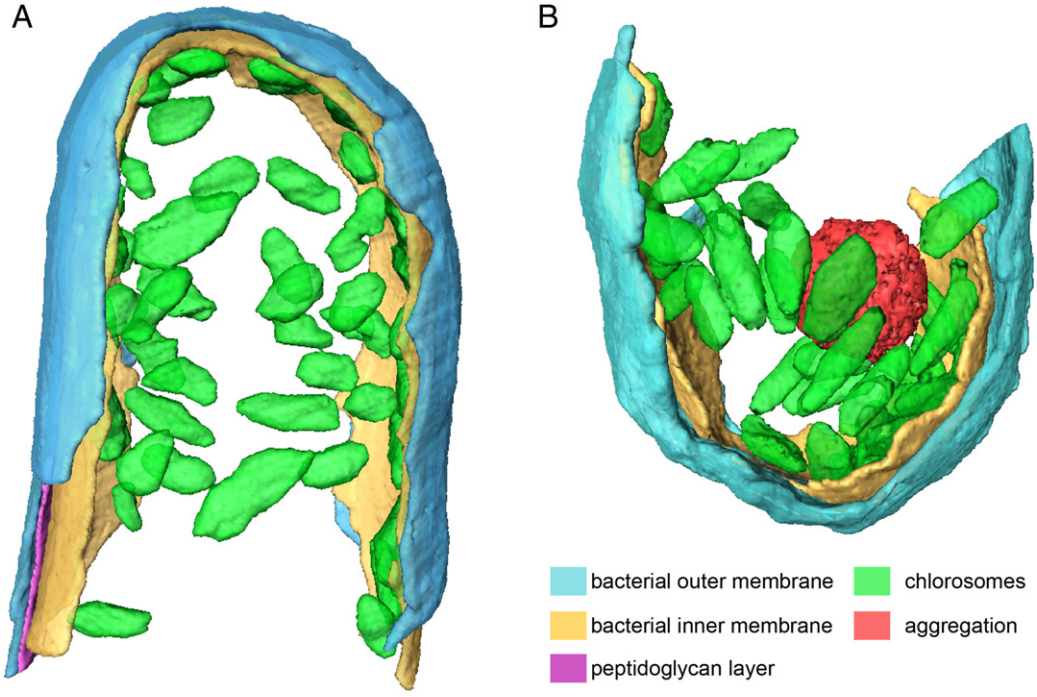

Fig. 3. Surface-rendered representation and intracellular chlorosome organization of *Cba tepidum* cells shown in Fig. 2. A) Cell cultured in the presence of S^{2-}, $S_2O_3^{2-}$. B) Cell cultured in the presence of S^{2-}.

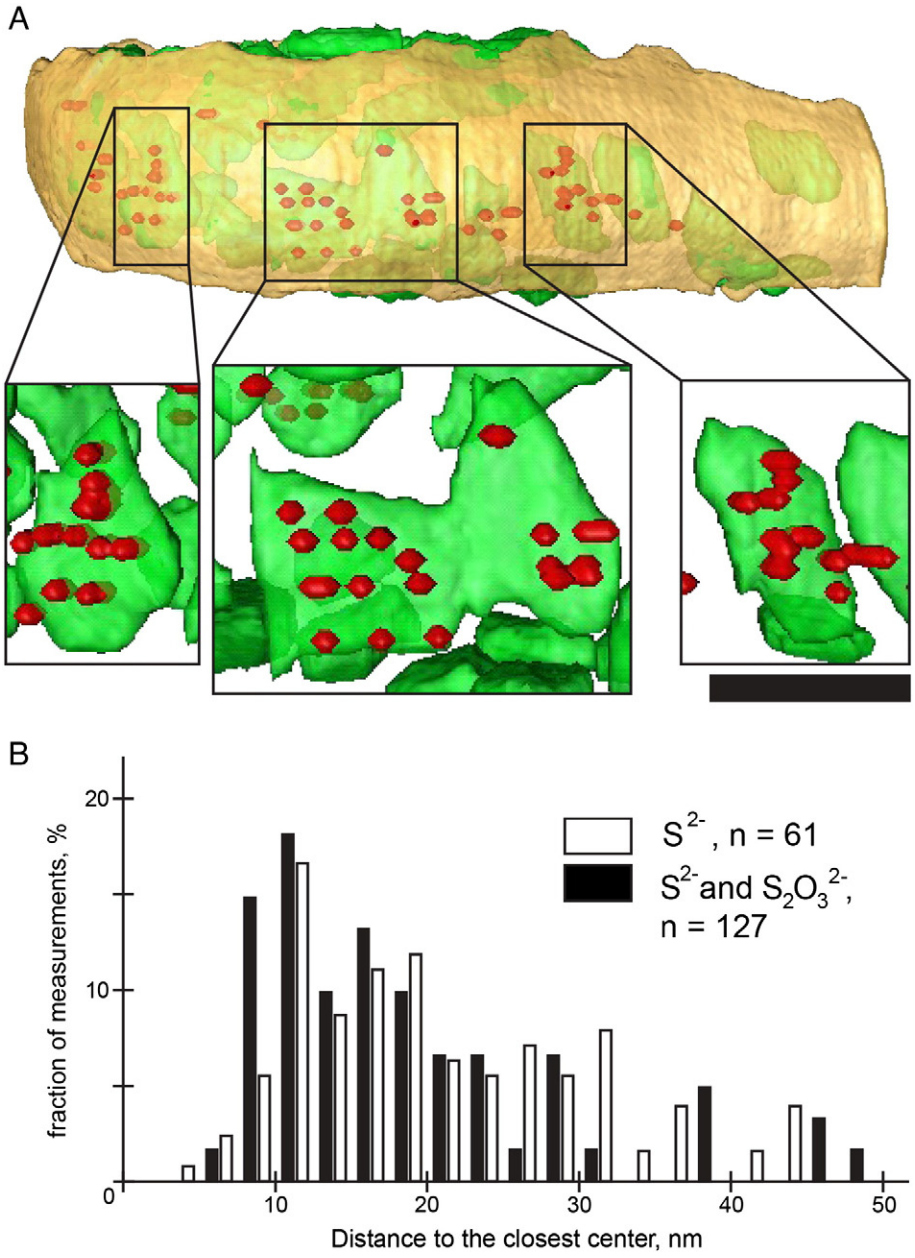

Fig. 4. Distribution of the RCs on the interface between the cytoplasmic membrane and chlorosomes. (A) Connections of the chlorosomes to the CM (red) in the *Cba tepidum* cell cultured in the presence of S^{2-} and $S_2O_3^{2-}$. Scale bar: 100 nm. (B) Histogram of distances between the RCs and their closest neighbors in nm. Measurements were made from 3 tomograms of bacteria cultured in the presence of S^{2-} and 8 tomograms of bacteria cultured in the presence of S^{2-} and $S_2O_3^{2-}$.

distribution (Fig. 5). Similarly a wide range of chlorosome dimensions have been previously observed with the AFM and EM of purified chlorosomes and chlorosomes within cell sections. Given the accuracy of cryo-ET to be in the order of nanometers, the range of chlorosome dimensions measured within one cell indicate genuine variations implying that the chlorosomes were at different stages of maturity since the size of chlorosomes is known to increase as they develop [46].

The precise means by which chlorosomes attach to the inner surface of the CM is still unknown. Their separation from this surface has been estimated as 2 nm by PFT-AFM [23]. The preparation examined did not contain sodium thiocyanate, which causes chlorosomes to dissociate from the CM. The CMs adsorbed to the mica surface were observed to have distinct globular protrusions, up to 30 nm wide and 6 nm high including the CM [23]. These are presumably different protein domains, but the resolution was limited. As shown in Fig. 2, cryo-ET allowed chlorosomes attached to membranes, to be directly imaged under close-to-native conditions. The center-to-center distance between the chlorosome envelope and the CM was 8.5 nm (Fig. 2F). This number includes a single membrane layer, which we estimate to be 2–3 nm, meaning that the gap between the CM and the chlorosome envelope is ~6 nm and must match with the height of the protein protrusions. This distance is close to the height of a single FMO protein trimer (5 nm) determined by X-ray analysis [10]. This value agrees better with the 6 nm height of the trimer FMO indicated by the 20 Å 3D map of the RC complex associated with FMO trimers [12]. Rather, the discrepancy of about 1.5 nm between our data and the X-ray data is consistent with linear dichroism experiments and mass spectrometry data, which suggest that the FMO protein is tilted between the CM and the chlorosomes [25,47]. As the 3D map of the FMO–RC complex shows that the FMO protein trimer interacts directly with the periphery of

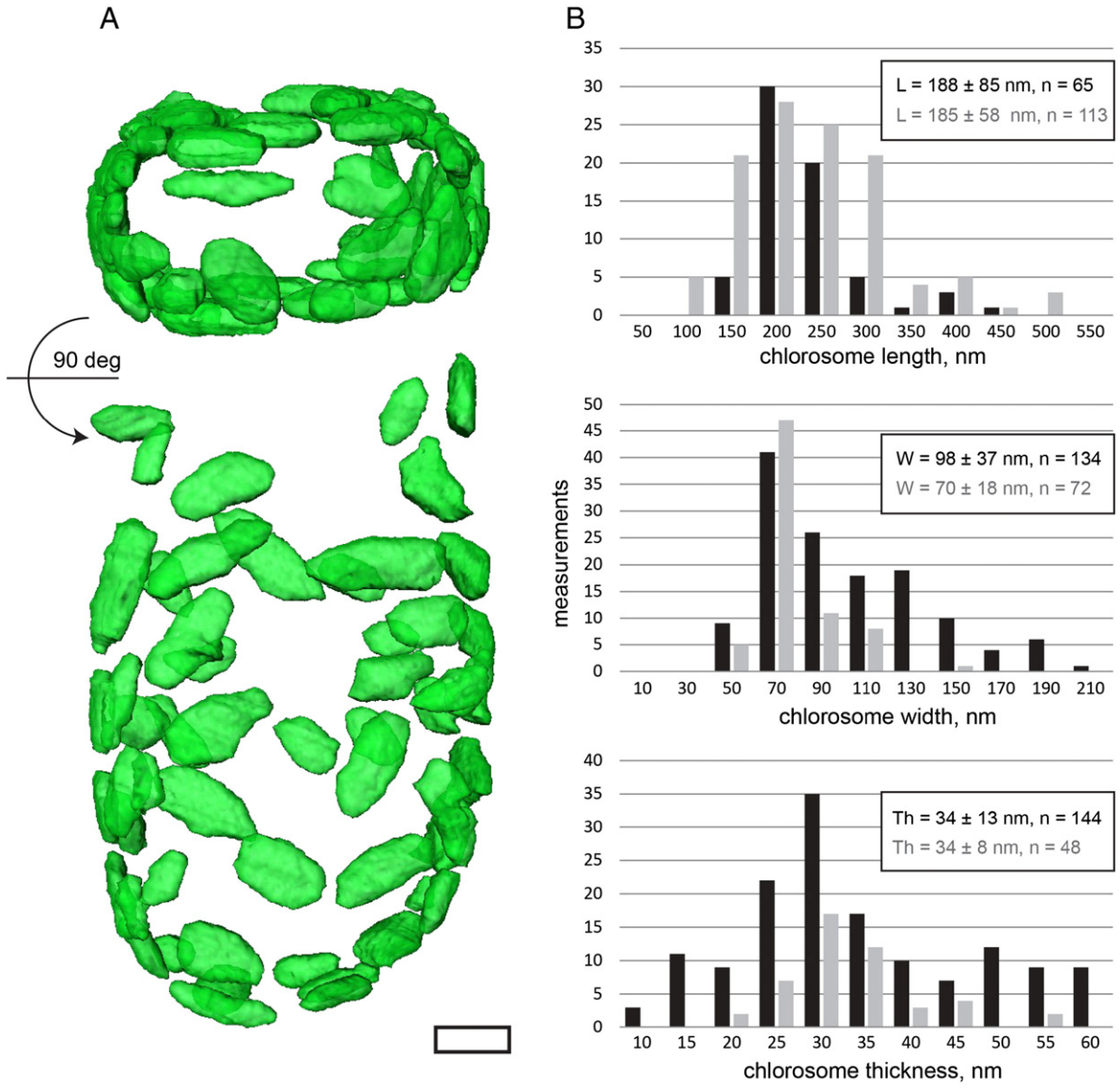

Fig. 5. Chlorosome dimensions. (A) A volume rendered representation showing the individual chlorosome organelles of a *Cba tepidum* cell cultured in the presence of S^{2-} and $S_2O_3^{2-}$. Bottom: the cell rotated 90°. Scale bar: 100 nm. (B) Chlorosome dimensions in cells cultured in the presence of S^{2-} and $S_2O_3^{2-}$ (black columns) or of S^{2-} (gray columns). The measurements were performed on all the recorded tomograms.

the PscA homodimer of the RC [12], the observed connections between the inner side of the CM and the chlorosomes precisely indicate the position of the RCs, allowing their distribution in the CM to be studied for the first time. The FMO of the RC are connected with the chlorosome *via* the CsmA protein of the chlorosomes. The CsmA binds BChl a and form an extensive paracrystalline baseplate. Although individual RCs are known to function alone [7,12,41], here we documented them as sometimes tightly packed at distances closer than 20 nm but not in regular arrangements.

Our results show that cryo-ET can be used to investigate chlorosomes in intact bacterial cells revealing their *in vivo* association with their native CM. Further studies are now required to examine bacteria at different growth stages or under different growth conditions to follow the maturation of chlorosomes and their envelope.

Acknowledgements

The authors thank Dr. S.A. Müller for the critical reading of the manuscript. The project was supported by the University of Crete (KA 3802), the Swiss National Foundation for Scientific Research (short term fellowship IZKOZ3_143001 to G.T.) and the Swiss Initiative for Systems Biology to MK and HS (SystemsX.ch, grant CINA).

References

[1] J. Overmann, The family *Chlorobiaceae*, in: M. Dworkin, S. Falkow, E. Rosenberg, K.-H. Schleifer, E. Stackebrandt (Eds.), The Prokaryotes: An Evolving Electronic Resource for the Microbiological Community, Springer Verlag, New York, 2000.
[2] J. Overmann, Ecology of phototrophic sulfur bacteria, in: R. Hell, C. Dahl, D.B. Knaff, T. Leustek (Eds.), Sulfur Metabolism in Phototrophic Organisms, Springer, Dordrecht, 2008, pp. 375–396.
[3] D.C. Brune, Sulfur compounds as photosynthetic electron donors, in: C.E. Bauer (Ed.), Anoxygenic Photosynthetic Bacteria, Kluwer, Amsterdam, 1995, pp. 847–870.
[4] L. Chan, T.S. Weber, R.M. Morgan-Kiss, T.E. Hanson, A genomic region required for phototrophic thiosulfate oxidation in the green sulfur bacterium *Chlorobium tepidum* (syn. *Chlorobaculum tepidum*), Microbiology 154 (2008) 818–829.
[5] H. Sakurai, T. Ogawa, M. Shiga, K. Inoue, Inorganic sulfur oxidizing system in green sulfur bacteria, Photosynth. Res. 104 (2010) 163–176.
[6] T.M. Wahlund, C.R. Woese, R.W. Castenholz, M.T. Madigan, A thermophilic green sulfur bacterium from New Zealand hot springs *Chlorobium tepidum* sp. nov, Arch. Microbiol. 156 (1991) 19–26.

[7] G. Hauska, T. Schoedl, H. Remigy, G. Tsiotis, The reaction center of green sulfur bacteria, Biochim. Biophys. Acta 1507 (2001) 260–277.
[8] J. Oelze, J.R. Golecki, Membrane and chlorosomes of green bacteria: structure, composition and development, in: R.E. Blankenship, M.T. Madigan, C.E. Bauer (Eds.), Anoxygenic Photosynthetic Bacteria, vol. 2, Kluwer Academic Publishers, Dordrecht/Boston/London, 1995, pp. 259–272.
[9] C.J. Law, A.W. Roszak, J. Southall, A.T. Gardiner, N.W. Isaacs, R.J. Cogdell, The structure and function of bacterial light-harvesting complexes, Mol. Membr. Biol. 21 (2004) 183–191.
[10] Y.F. Li, W. Zhou, R.E. Blankenship, J.P. Allen, Crystal structure of the bacteriochlorophyll a protein from *Chlorobium tepidum*, J. Mol. Biol. 271 (1997) 456–471.
[11] H. Remigy, D. Fotiadis, B. Wolpensinger, S.A. Mueller, A. Engel, G. Tsiotis, Evidence for the association of three FMO subunits per reaction center of *Chlorobium tepidum* by scanning transmission electron microscopy, in: G. Garab (Ed.), Photosynthesis: Mechanisms and Effects, vol. I, 1998, pp. 531–534.
[12] H.W. Remigy, H. Stahlberg, D. Fotiadis, S.A. Muller, B. Wolpensinger, A. Engel, G. Hauska, G. Tsiotis, The reaction center complex from the green sulfur bacterium *Chlorobium tepidum*: a structural analysis by scanning transmission electron microscopy, J. Mol. Biol. 290 (1999) 851–858.
[13] G.T. Oostergetel, H. van Amerongen, E.J. Boekema, The chlorosome: a prototype for efficient light harvesting in photosynthesis, Photosynth. Res. 104 (2010) 245–255.
[14] R.E. Blankenship, K. Matsuura, Antenna complexes from green photosynthetic bacteria, in: B.R. Green, W.W. Parson (Eds.), Light-harvesting Antenna in Photosynthesis, Kluwer Academic Publishers, Dordrecht, The Netherlands, 2003, pp. 195–217.
[15] N.-U. Frigaard, D.A. Bryant, Chlorosomes: antenna organelles in green photosynthetic bacteria, in: J.M. Shively (Ed.), Complex Intracellular Structures in Prokaryotes in Microbiology Monographs, vol. 2, Springer-Verlag, Berlin, 2006, pp. 79–114.
[16] M.Ø. Pedersen, J. Linnanto, N.U. Frigaard, N.C. Nielsen, M. Miller, A model of the protein–pigment baseplate complex in chlorosomes of photosynthetic green bacteria, Photosynth. Res. 104 (2010) 233–243.
[17] G. Tsiotis, C. Hager-Braun, B. Wolpensinger, A. Engel, G. Hauska, Structural analysis of the photosynthetic reaction center from the green sulfur bacterium *Chlorobium tepidum*, Biochim. Biophys. Acta 1322 (1997) 163–172.
[18] K. Kouyianou, P.J. De Bock, S.A. Müller, A. Nikolaki, A. Rizos, V. Krzyžánek, A. Aktoudianaki, J. Vandekerckhove, A. Engel, K. Gevaert, G. Tsiotis, The chlorosome of *Chlorobaculum tepidum*: mass, size and protein composition revealed by electron microscopy, dynamic light scattering and mass spectrometry-driven proteomics, Proteomics 11 (2011) 2867–2880.
[19] D.E. Tronrud, M.F. Schmid, B.W. Matthews, Structure and X-ray amino acid sequence of a bacteriochlorophyll a protein from *Prosthecochloris aestuarii* refined at 1.9 A resolution, J. Mol. Biol. 188 (1986) 443–454.
[20] G.T. Oostergetel, M. Reus, A. Gomez Maqueo Chew, D.A. Bryant, E.J. Boekema, A.R. Holzwarth, Long-range organization of bacteriochlorophyll in chlorosomes of *Chlorobium tepidum* investigated by cryo-electron microscopy, FEBS Lett. 581 (2007) 5435–5439.
[21] J. Psencík, A.M. Collins, L. Liljeroos, M. Torkkeli, P. Laurinmäki, H.M. Ansink, T.P. Ikonen, R.E. Serimaa, R.E. Blankenship, R. Tuma, S.J. Butcher, Structure of chlorosomes from the green filamentous bacterium *Chloroflexus aurantiacus*, J. Bacteriol. 191 (2009) 6701–6708.
[22] J. Psencík, T.P. Ikonen, P. Laurinmäki, M.C. Merckel, S.J. Butcher, R.E. Serimaa, R. Tuma, Lamellar organization of pigments in chlorosomes, the light harvesting complexes of green photosynthetic bacteria, Biophys. J. 87 (2004) 1165–1172.
[23] P.G. Adams, A.J. Cadby, B. Robinson, Y. Tsukatani, M. Tank, J. Wen, R.E. Blankenship, D.A. Bryant, C.N. Hunter, Comparison of the physical characteristics of chlorosomes from three different phyla of green phototrophic bacteria, Biochim. Biophys. Acta 1827 (2013) 1235–1244.
[24] M.F. Hohmann-Marriott, R.E. Blankenship, R.W. Roberson, The ultrastructure of *Chlorobium tepidum* chlorosomes revealed by electron microscopy, Photosynth. Res. 86 (2005) 145–154.
[25] J. Wen, H. Zhang, M.L. Gross, R.E. Blankenship, Membrane orientation of the FMO antenna protein from *Chlorobaculum tepidum* as determined by mass spectrometry-based footprinting, Proc. Natl. Acad. Sci. U. S. A. 106 (2009) 6134–6139.
[26] L.A. Staehelin, J.R. Golecki, G. Drews, Supramolecular organization of chlorosomes (chlorobium vesicles) and of their membrane attachment sites in *Chlorobium limicola*, Biochim. Biophys. Acta 589 (1980) 30–45.
[27] M.F. Hohmann-Marriott, R.W. Roberson, Exploring photosynthesis by electron tomography, Photosynth. Res. 102 (2009) 177–188.
[28] V. Lučič, A. Rigort, W. Baumeister, Cryo-electron tomography: the challenge of doing structural biology in situ, J. Cell Biol. 202 (2013) 407–419.
[29] L.J. Stal, H. van Gemerden, W.E. Krumbein, The simultaneous assay of chlorophyll and bacteriochlorophyll in natural microbial communities, J. Microbiol. Methods 2 (1984) 295–306.
[30] R.Y. Stanier, J.H.C. Smith, The chlorophylls of green bacteria, Biochim. Biophys. Acta 41 (1960) 478–484.
[31] J.D. Cline, Spectrophotometric determination of hydrogen sulfide in natural waters, Limnol. Oceanogr. 14 (1969) 454–458.
[32] M. Kudryashev, S. Münter, L. Lemgruber, G. Montagna, H. Stahlberg, K. Matuschewski, M. Meissner, M. Cyrklaff, F. Frischknecht, Structural basis for chirality and directional motility of *Plasmodium* sporozoites, Cell. Microbiol. 14 (2012) 1757–1768.
[33] J.R. Kremer, D.N. Mastronarde, J.R. McIntosh, Computer visualization of three-dimensional image data using IMOD, J. Struct. Biol. 116 (1996) 71–76.
[34] D. Castaño-Díez, M. Kudryashev, M. Arheit, H. Stahlberg, Dynamo: a flexible, user-friendly development tool for subtomogram averaging of cryo-EM data in high-performance computing environments, J. Struct. Biol. 178 (2012) 139–151.
[35] M. Kudryashev, D. Castano-Diez, H. Stahlberg, Limiting factors in single particle cryo electron tomography, Comput. Struct. Biotech. J. 1 (2012).
[36] T. Cavalier-Smith, Obcells as proto-organisms: membrane heredity, lithophosphorylation, and the origins of the genetic code, the first cells, and photosynthesis, J. Mol. Evol. 53 (2001) 555–595.
[37] A. Prange, R. Chauvistre, H. Modrow, J. Hormes, H.G. Truper, C. Dahl, Quantitative speciation of sulfur in bacterial sulfur globules: X-ray absorption spectroscopy reveals at least three different species of sulfur, Microbiology 148 (2002) 267–276.
[38] H. van Gemerden, Production of elemental sulfur by green and purple sulfur bacteria, Arch. Microbiol. 146 (1986) 52–56.
[39] J.A. Eisen, K.E. Nelson, I.T. Paulsen, J.F. Heidelberg, M. Wu, R.J. Dodson, R. Deboy, M.L. Gwinn, W.C. Nelson, D.H. Haft, E.K. Hickey, J.D. Peterson, A.S. Durkin, J.L. Kolonay, F. Yang, I. Holt, L.A. Umayam, T. Mason, M. Brenner, T.P. Shea, D. Parksey, W.C. Nierman, T.V. Feldblyum, C.L. Hansen, M.B. Craven, D. Radune, J. Vamathevan, H. Khouri, O. White, T.M. Gruber, K.A. Ketchum, J.C. Venter, H. Tettelin, D.A. Bryant, C. M. Fraser, The complete genome sequence of *Chlorobium tepidum* TLS, a photosynthetic, anaerobic, green-sulfur bacterium, Proc. Natl. Acad. Sci. U. S. A. 99 (2002) 9509–9514.
[40] L.H. Gregersen, D.A. Bryant, N.U. Frigaard, Mechanisms and evolution of oxidative sulfur metabolism in green sulfur bacteria, Front. Microbiol. (2011), http://dx.doi.org/10.3389/fmicb.2011.00116.
[41] H.W. Rémigy, G. Hauska, S.A. Müller, G. Tsiotis, The reaction centre from green sulphur bacteria: progress towards structural elucidation, Photosynth. Res. 71 (2002) 91–98.
[42] S. Ganapathy, G.T. Oostergetel, P.K. Wawrzyniak, M. Reus, A. Gomez Maqueo Chew, F. Buda, E.J. Boekema, D.A. Bryant, A.R. Holzwarth, H.J.M. de Groot, Alternating syn-anti bacteriochlorophylls form concentric helical nanotubes in chlorosomes, Proc. Natl. Acad. Sci. U. S. A. 106 (2009) 8525–8530.
[43] J.R. Golecki, J. Oelze, Quantitative relationships between bacteriochlorophyll content, cytoplasmic membrane structure and chlorosome size in *Chloroflexus aurantiacus*, Arch. Microbiol. 148 (1987) 236–241.
[44] A. Martinez-Planells, J.B. Arellano, C.M. Borrego, C. Lopez-Iglesias, F. Gich, J. Garcia-Gil, Determination of the topography and biometry of chlorosomes by atomic force microscopy, Photosynth. Res. 71 (2002) 83–90.
[45] Z.-Y. Wang, G. Marx, M. Umetsu, M. Kobayashi, M. Mimuro, T. Nozawa, Morphology and spectroscopy of chlorosomes from *Chlorobium tepidum* by alcohol treatments, Biochim. Biophys. Acta Bioenerg. 1232 (1995) 187–196.
[46] M. Foidl, J.R. Golecki, J. Oelze, Chlorosome development in *Chloroflexus aurantiacus*, Photosynth. Res. 55 (1998) 109–114.
[47] A.N. Melkozernov, J.M. Olson, Y.F. Li, J.P. Allen, R.E. Blankenship, Orientation and excitonic interactions of the Fenna–Matthews–Olson protein in membranes of the green sulfur bacterium *Chlorobium tepidum*, Photosynth. Res. 56 (1998) 315–328.
[48] G.A. Montaño, B.P. Bowen, J.T. LaBell, N.W. Woodbury, V.B. Pizziconi, R.E. Blankenship, Characterization of Chlorobium tepidum chlorosomes: a calculation of bacteriochlorophyll c per chlorosome and oligomer modeling, Biophys. J. 85 (2003) 2560–2565.